

## **General Disclaimer**

### **One or more of the Following Statements may affect this Document**

- This document has been reproduced from the best copy furnished by the organizational source. It is being released in the interest of making available as much information as possible.
- This document may contain data, which exceeds the sheet parameters. It was furnished in this condition by the organizational source and is the best copy available.
- This document may contain tone-on-tone or color graphs, charts and/or pictures, which have been reproduced in black and white.
- This document is paginated as submitted by the original source.
- Portions of this document are not fully legible due to the historical nature of some of the material. However, it is the best reproduction available from the original submission.

MICROANALYTICAL IDENTIFICATION OF BARIUM SULPHATE CRYSTALS IN  
STATOLITHS OF CHARA RHIZOIDS (CHARA FRAGILIS, DESV.)

Klaus Schröter, Andre Lächli, and Andreas Sievers

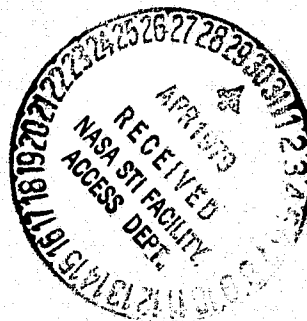
Translation of "Mikroanalytische Identifikation von Barium-  
sulfat-Kristallen in den Statolithen der Rhizoide von Chara  
fragilis, Desv.," Planta (Berlin) Vol. 122, 1975, pp. 213-225.

(NASA-TM-75611) MICROANALYTICAL  
IDENTIFICATION OF BARIUM SULPHATE CRYSTALS  
IN STATOLITHS OF CHARA RHIZOIDS (National  
Aeronautics and Space Administration) 19 p  
HC A02/MF A01

N79-21744

Unclas  
20262

CSSL 06C G3/51



MICROANALYTICAL IDENTIFICATION OF BARIUM SULFATE CRYSTALS IN  
STATOLITHS OF CHARA RHIZOIDS (CHARA FRAGILIS, DESV.)<sup>1</sup>

Klaus Schröter, Andre Läuchli,<sup>2</sup> and Andreas Sievers  
Botanical Institute of the University of Bonn, West Germany

Summary: In contrast to the statocytes of higher plants, /213\* in which amyloplasts function as statoliths, Chara rhizoids contain statolith vacuoles filled with biocrystallites of BaSO<sub>4</sub>. This was revealed by qualitative and quantitative electron microprobe analysis, atomic absorption spectrophotometry and selected area electron diffraction. The barium sulfate crystallites are rods which are linearly composed of globular subunits approximately 7 nm in diameter.

The electron optical evidence of the crystallites depends on the nature of the fixatives. Best structural preservation was observed after fixation in a buffered solution of glutaraldehyde plus acrolein without addition of heavy metals. OsO<sub>4</sub> and particularly KMnO<sub>4</sub> partially dissolve the biocrystallites as well as synthetic BaSO<sub>4</sub>. The crystal solubility must be taken into consideration when micrographs of such small crystallites are interpreted.

The fact that BaSO<sub>4</sub> is chemically very inert seems to exclude biochemical interactions of the statoliths with other cell components during graviperception. It favors the theory that only the mass of the statoliths is effective.

---

<sup>1</sup> Expanded partial reprint from a dissertation by K. S[chröter]. Research was furthered by material grants from the Deutsche Forschungsgemeinschaft to A. S[ievers].

<sup>2</sup> Botanical Institute of the Technical University of Darmstadt.

\* Numbers in the margins indicate pagination in the foreign text.

## 1. Introduction

In considerations on the mechanism of the stimulus-response chain in positively geotropic Chara rhizoids [Sievers and Schröter, 1971], the question of the chemical nature of the statoliths has remained unanswered. Because of their sharp light-optical contrast they were first called "shiny bodies" [Zacharias 1889]. Color reagents for organic compounds, especially including starch, yielded either ambiguous results or none at all.

Under the electron microscope the statoliths proved to be not amyloplasts, but bodies enclosed in special vacuoles and containing (in addition to a fibrillary basic substance) numerous radially arranged rod-shaped particles [Sievers 1965, 1967]. These particles are conspicuous for their sharp electron-optical contrast. The contrast is thus not based on a deposition of metal atoms during preparation [Schröter et al. 1973].

/214

The question of the chemical nature of these statoliths particularly concerns a determination whether the statoliths contain or can produce substances which affect the geotropic reaction of the rhizoids, or whether the statoliths are instead chemically inert and act only by virtue of their mass.

## 2. Materials and Method

On the cultivation of Chara rhizoids cf. Sievers [1965].

### 2.1. Transmission Electron Microscopy

Fixation: a) 1% glutaraldehyde and 0.3% acrolein in 0.05 M Na-cacodylate buffer solution (NCP), 2 hrs. at room temperature. If fixed a second time: 1.5% OsO<sub>4</sub> om 0.05 M NCP, 2 hrs. at 4°C.  
b) 2% KMnO<sub>4</sub> at room temperature, 2 hrs. or 5 mins. Embedding in araldite, microtomization with the Reichert Om U-2. Section contrasting with uranyl acetate and lead citrate (only in Fig. 8).

Microscopy with the Siemens "Elmiskop" IA and 101.

## 2.2. X-Ray Microanalysis

The study was performed with air-dried rhizoids and ca. 1- $\mu$ m sections from the statolith zone of aldehyde-fixed rhizoids, the latter embedded in araldite. To raise electrical and thermic conductivity an aluminum coating ca. 10 nm thick was vaporized onto both sides of the support films carrying the objectives. Examination followed with a CAMECA microsoud. Acceleration voltage was 30 kV. On the method of x-ray microanalysis of plant specimens cf. Lhuchli [1972].

The energy-dispersive x-ray spectrum was evaluated for qualitative analysis (EDAX system).

For quantitative analysis, two PET crystal spectrometers were used, set for barium  $L_{\alpha}$  and sulfur  $K_{\alpha}$  radiation. Measurement time was 10 and 40 sec., respectively. The impulse counts from various measurements and samples were compared [Skaer et al. 1974]

## 2.3. Atomic Absorption Spectrophotometer

Several samples with ca. 60 rhizoid points were dried on parafilm in air. Evaluation with a Beckman atomic absorption spectrophotometer 448, equipped with a Massmann cell. Barium lamp 553.6 nm. Work program: (1) drying 20 sec., 110°C; (2) incineration 40 sec., 1,100°C; (3) measurement phase 10 sec., 2,600°C; (4) bakeout 10 sec., 3,000°C.

## 3. Results

### 3.1. Crystal Structure of the Statoliths

As a rule a statolith compartment has only one included body (Fig. 1, St). Even with light microscopy, the vacuole/plasma /216 phase boundary can be recognized (►). If rhizoids are heated for 30 min. at 850°C, only carbonized residues (R) of the organic cell

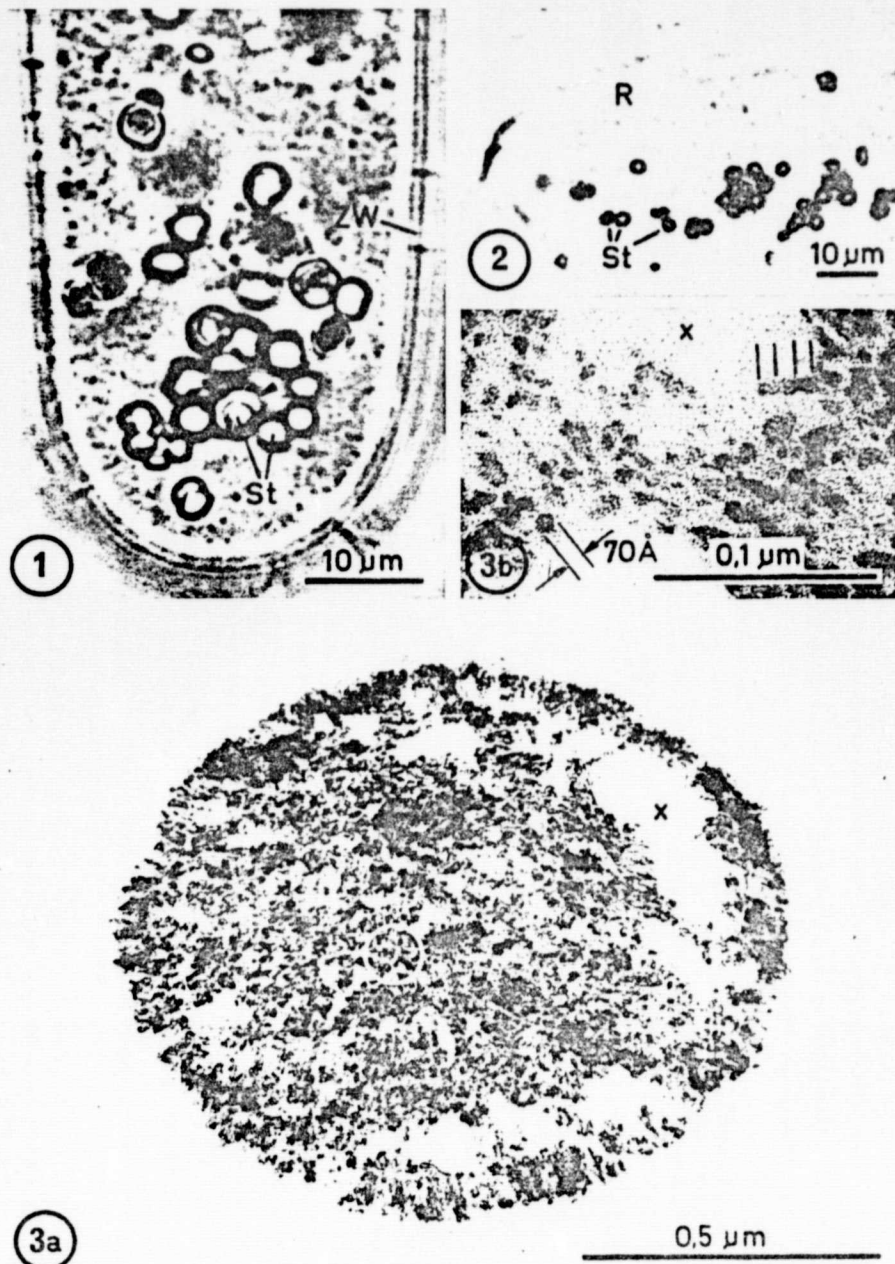


Fig. 1. Apical part of a live *Chara* rhizoid (horizontal position, photographed from above). The statoliths (St), mostly isolated, lie in specific vacuoles. The vacuole/plasma phase boundary is clearly visible (►). ZW = cell wall. Light microscopy 1600:1.

Fig. 2. Apical part of an incinerated rhizoid. If a rhizoid is heated for 30 min. at 850°C, all organic components are carbonized (R). The statoliths (St), however, hardly change form or size. Light microscopy 800:1

/215

Figs. 3a and b. Cross section of a statolith containing crystallites in situ. Because of the tangential direction of cutting, longer crystallites are present only around the periphery, while the center (circle) presents round crystallite sections (a) with a diameter of ca. 7 nm (b). The hardness of the crystallites frequently leads to cutting artifacts: Flawed points at (x). Aldehyde fixation without addition of metals. (a) 80,000:1. (b) 300,000:1.

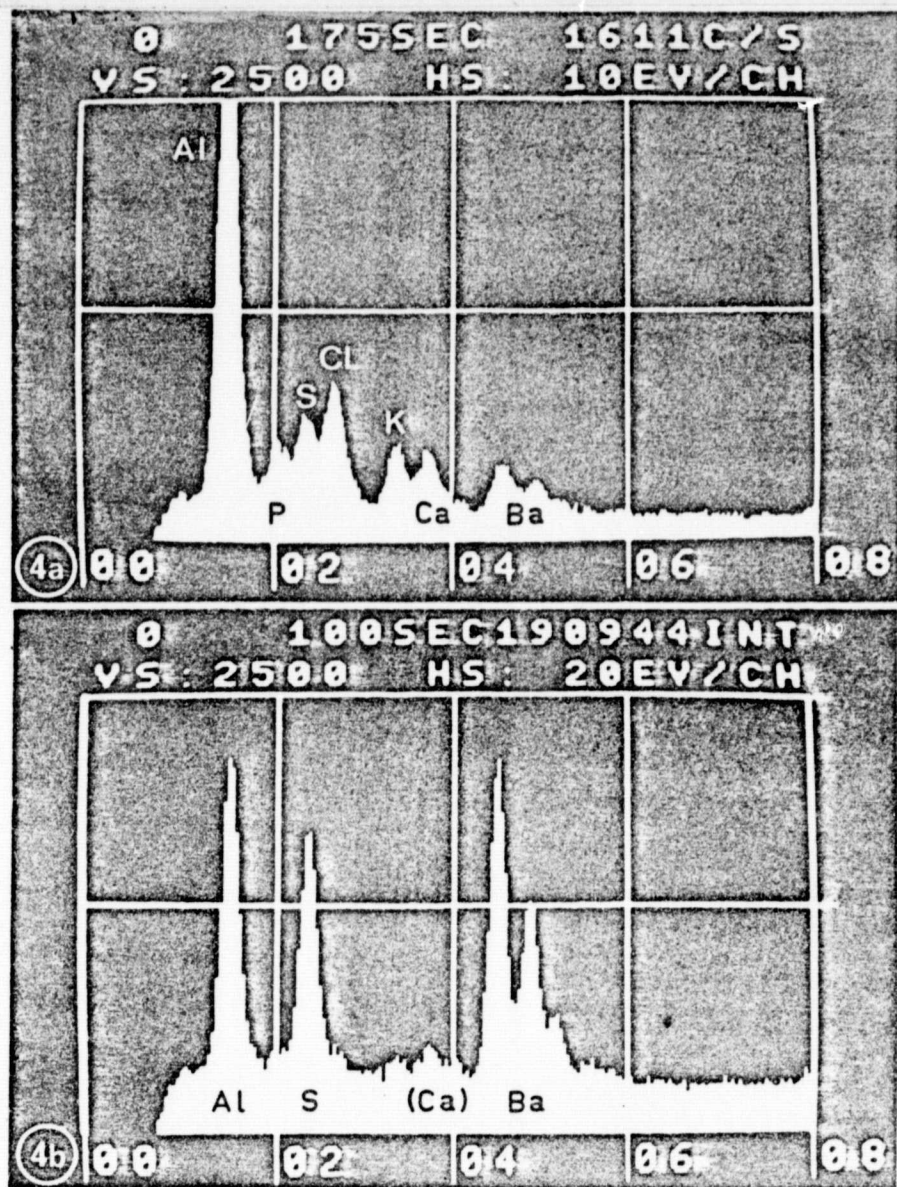
components can be recognized, while the form and light diffraction of the statoliths (St) seem almost unaltered (Fig. 2, cf. also [Zacharias, 1889]). The heat resistance indicates an inorganic-crystalline content of the statoliths, which is also expressed by the sharp electron-optical inherent contrast of the statolith particles (Fig. 3a). Since the picture contrast at a medium acceleration voltage (80 kV) and a small aperture (20  $\mu\text{m}$ ) is essentially caused by mass thickness ( $\rho D$ ,  $\rho$  = density,  $D$  = thickness of section) and less so by the greater dispersion capacity of atoms with higher atomic numbers [Reimer, 1967], the density ( $\rho$ ) of the particles must be greater than that of the surrounding structures. This is the case only with crystals.

The statolith crystals were described by Sievers [1967] and Schröter et al. [1972] as rod-shaped particles radially arranged in relation to the center of the statolith. Figure 3a shows a tangentially cut section from a statolith, in the center of which almost circular crystallites are recognizable. These are cross-sections of the radially arranged crystallites. Their diameter is around 7 nm (Fig. 3b). The hardness of the crystals and the small distance between them often lead to cutting artifacts: statolith material breaks out (x). The spherical to ellipsoidal form of the statoliths causes cutting pictures that present longer crystallites only in the periphery. According to the available picture material the length varies sharply. Individual crystallites are up to 150 nm long. The rod-shaped solitary crystals, however, are not homogeneous. One can almost always recognize isodiametrical subunits with a diameter of ca. 7 nm. Figure 3b contains a solitary crystal consisting of three subunits.

### 3.2. Microanalysis

Using energy dispersion x-ray microanalysis the elements phosphorus, sulfur, chlorine, potassium, calcium and barium can be detected in the microvolume in and above the statoliths of dried rhizoids (Fig. 4a). As a result of the preparation (cf. Method)

ORIGINAL PAGE IS  
OF POOR QUALITY



(/217)

Fig. 4. Energy-dispersion x-ray spectrum of a total preparation (a: dried mass of rhizoid cell wall, cytoplasm and statolith) and a single aldehyde-fixed statolith (b). Both preparations were vapor-coated with aluminum. The spectrum of the total preparation (a) contains the maximums (theoretical values) of 7 elements: Al  $K_{\alpha}$  (1.486 keV), P  $K_{\alpha}$  (2.013 keV), S  $K_{\alpha}$  (2.307 keV), Cl  $K_{\alpha}$  (2.621 keV), K  $K_{\alpha}$  (3.312 keV), Ca  $K_{\alpha}$  (3.690 keV), Ba  $L_{\alpha}$  (4.465 keV), Ba  $L_{\beta 1}$  (4.827 keV), Ba  $L_{\beta 2}$  (5.193 keV). In the cutting preparation (b) only S and Ba can be detected, in addition to Al.

the minimum is also present. If, in contrast to the total preparation, the statolith content alone is analyzed, then in addition to aluminum only sulfur and barium can be identified. Figure 4b



shows the sound graph of a statolith fixed with aldehyde. Sulfur is represented with its  $K_{\alpha}$  maximum, barium with the  $L_{\alpha}$ ,  $L_{\beta 1}$  and  $L_{\beta 2}$  maximums. Further elements are not significantly distinct from the background. Elements with low atomic numbers, including carbon and oxygen, are routinely undetectable with an x-ray microsound.

In a quantitative x-ray microanalysis the ratio of barium to sulfur (Ba/S) in the statolith crystals was determined. As a standard Ba - S compound with a 1:1 atomic ratio of Ba to S, let us use chemically stable  $BaSO_4$ .

/218

Table 1 contains the impulse counts (P) of the barium and sulfur maximums, corrected for background radiation (b) [Skaer et al 1974], and also the ratio of the corrected impulse counts of barium and sulfur.  $(P - b)_{Ba} / (P - b)_S$ . As a result of the dif-

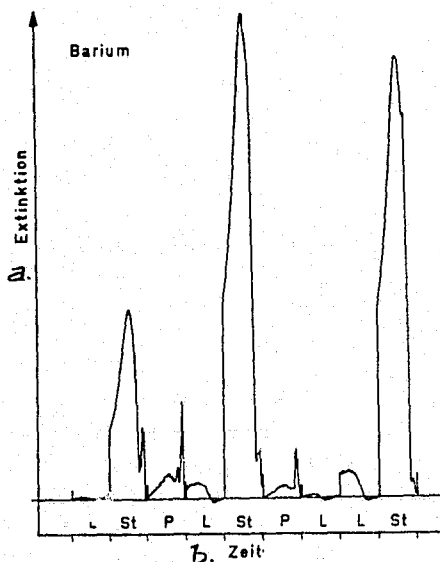
Table 1. Results of quantitative x-ray microanalysis

Synthetic $BaSO_4$			Statoliths (prepared sections, 1 $\mu m$ thick)			Rhizoid apex (dried total prepara- tions without stato- liths)	
Ba (P-b)	S (P-b)	$\frac{(P-b)_{Ba}}{(P-b)_S}$	Ba (P-b)	S (P-b)	$\frac{(P-b)_{Ba}}{(P-b)_S}$	Ba (P-b)	S (P-b)
865	349	2.48	1898	668	2.48	61	608
746	211	3.54	4895	1468	3.33	77	561
626	196	3.19	868	354	2.45	92	729
808	283	2.86	2473	794	3.12	53	476
1237	367	3.37	913	350	2.61		
807	260	3.10	3152	1114	2.83		
848	312	2.72	4456	1393	3.20		
612	191	3.20	737	320	2.30		
1263	467	2.70	5074	1631	3.11		
685	268	2.56	2238	779	2.87		
measurement time: 40 s			measurement time: 40 s			measurement time: 40 s (P - b) corrected impulse count	
avg. $\frac{(P-b)_{Ba}}{(P-b)_S}$			avg. $\frac{(P-b)_{Ba}}{(P-b)_S}$				
2.97 (s = $\pm 0.36$ , n = 10)			2.86 (s = $\pm 0.34$ , n = 10)				

ORIGINAL PAGE IS  
OF POOR QUALITY

fering Ba or S contents in the microvolumes studied, the impulse counts for the individual samples differ for barium and sulfur. In a comparison of impulse counts between statolith and synthetic  $BaSO_4$  the differing measurement time must also be taken into account (10 compared to 40 sec.). The impulse count quotients, however, are sufficiently equal (statolith:  $2.86 \pm 0.34$ ,  $n = 10$ ; standard:  $2.97 \pm 0.36$ ,  $n = 10$ ). The barium - sulfur ratio in biogenic crystals is thus almost identical to that of synthetic  $BaSO_4$  crystals. In the dry rhizoid cytoplasm and cell wall masses, barium is detectable by only a few impulses.

The presence of barium in the statoliths was confirmed with barium extinction measurements in an atomic absorption spectrophotometer (Fig. 5). The graph contains only the measurement phases (abscissa). Previously the apparatus was calibrated

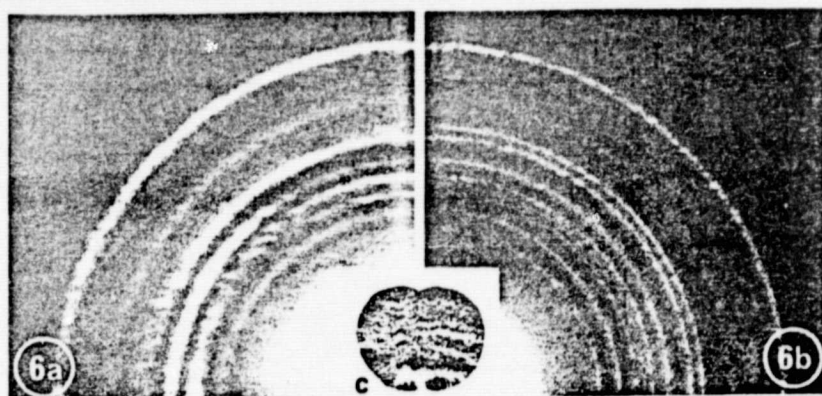


Key: \*  
a. extinction  
b. time

with freshly precipitated barium sulfate. Three samples (St) with different statolith contents are the basis for the high maximums. In between, blank samples (L) were included as well as two samples of parafilm (P) on which the air-dried rhizoid tips were brought to the evaporation chamber.

Fig. 5. Barium extinction curves of statoliths measured with atomic absorption spectrophotometer and recorder. Three statolith samples of different sizes were evaluated (St), and two parafilm samples (P) (the statoliths were on parafilm), and several blanks (L). Extinction was measured for 10 sec. during sample incineration.

Electron diffraction graphs of the statolith crystallites led to a clarification of crystallite structure. Figure 6a shows a quadrant of the fine-range diffraction graph of the statolith seen in Fig. 6c. Since the crystallites are



Figs. 6a - c. Fine range diffraction graphs of a statolith (a) shown in (c) and of a suspension preparation of freshly precipitated  $\text{BaSO}_4$  (b). The preferably radial orientation of the crystallites in the statolith leads to deviations in the intensity of individual diffraction rings (a). (b) photo: H.R. Oswald and A. Portmann. (c) aldehyde fixation without addition of metals. 10,000:1.

spatially oriented and not distributed at random, one gets not a balanced ring graph but symmetrical variations in intensity within individual diffraction rings. /219

The interlatticeplane distances (d) of the statolith crystals, calculated from the radii of the diffraction rings [Deloge and Cadot 1972], were compared with the d values of all Ba - S compounds in the ASTA file<sup>1</sup>, especially the d-values of those compounds with Ba - S ratios of 1:1. The comparison shows that the lattice values of the barium sulfate crystals ( $\text{BaSO}_4$ ,  $\beta$  type) are largely identical to the values of the statolith crystals. A comparison graph of freshly precipitated  $\text{BaSO}_4$  can be seen in Fig. 6b. The crystals of the synthetic sample are statistically evenly arranged and thus, in comparison to the biogenic material, (Fig. 6a), yield whole diffraction rings. The two electron diffraction graphs are

<sup>1</sup> Inorganic Index to the Powder Diffraction File of the American Society for Testing Materials.

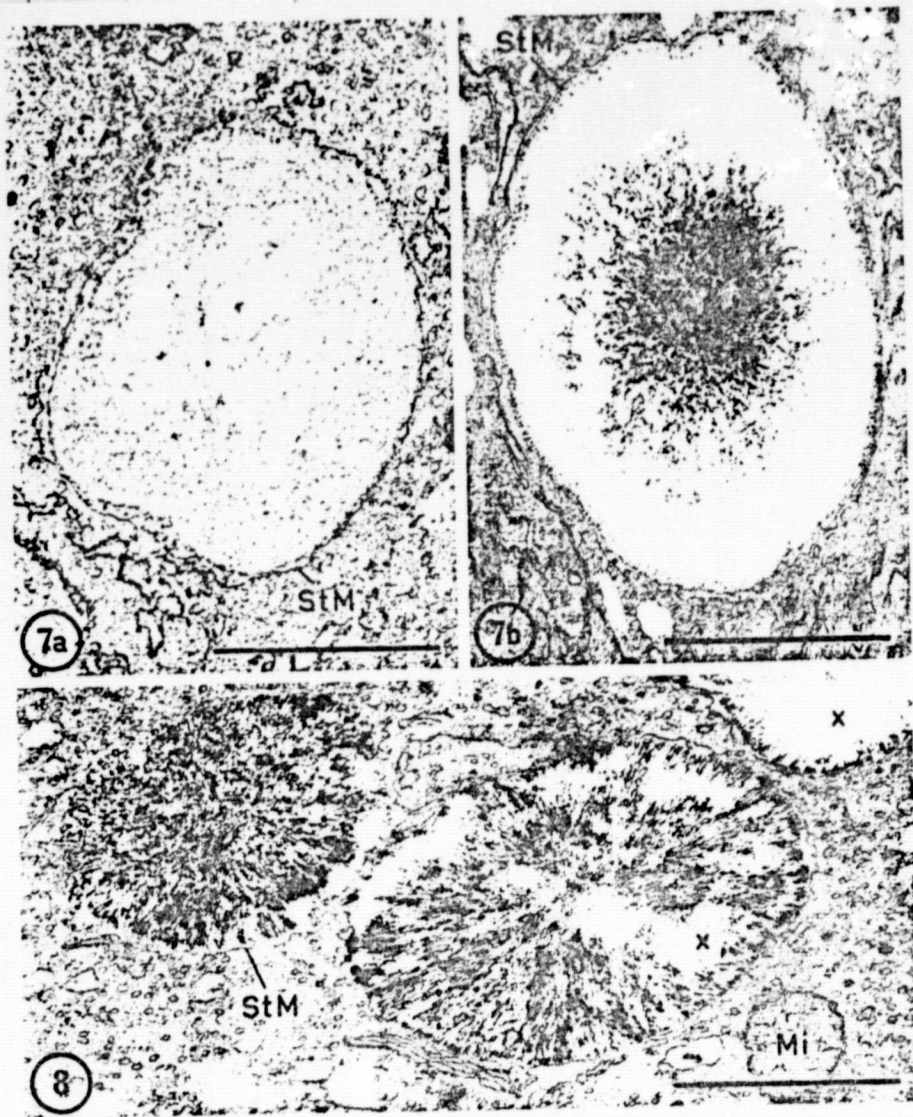


Fig. 7a and b. Cross sections of statoliths. Electron microscopic detection of crystallites after fixation with  $\text{KMnO}_4$  (2%) is possible only after very short fixing times (a: no crystallites after 2 hrs. b: crystallites concentrated in the center after 5 min.). The statolith crystallite content decreases first around the periphery. StM = statolith membrane.  $\text{KMnO}_4$  fixation. Mark = 1  $\mu\text{m}$ . 30,000:1.

Fig. 8. Cross section of statoliths. In contrast to Fig. 7, statoliths prefixed with aldehyde for 2 hrs. and subsequently fixed with  $\text{OsO}_4$  in cold ( $4^\circ\text{C}$ ) for 2 hrs. are full of crystallites. x = artificial flaw. Mi = mitochondrion. StM = statolith membrane. Aldehydr -  $\text{OsO}_4$  fixation. Mark = 1  $\mu\text{m}$ . 30,000:1.

ORIGINAL PAGE IS  
OF POOR QUALITY

ORIGINAL PAGE IS  
OF POOR QUALITY

in excellent agreement, including for the ring intensities which deviate in part from the x-ray values of the ASTM file.

### 3.3. The Effects of Fixing Reagents on the Solubility of Biogenic and Synthetic BaSO<sub>4</sub> Crystallites

The first electron microscope photographs of Chara statoliths after fixation in 2% KMnO<sub>4</sub> solution presented an almost structureless inclusive body inside the statolith membrane; it is bounded by a precipitate membrane (Fig. 7a [Sievers 1965]). The electron-impermeable crystallites could only be arrived at after fixation /220 with osmium (VIII) oxide (2% OsO<sub>4</sub> [Sievers 1967]). However, the crystallite content thus presented in the electron microscope varies from statolith to statolith. After fixing with aldehydes and subsequently also with OsO<sub>4</sub> (Fig. 8, cf. also Sievers 1967) one gets structures with a more constant crystallite content. The most crystallites are presented by statoliths fixed exclusively with aldehydes (Fig. 3).

The representability of statolith crystallites is thus clearly dependent on the fixative used. The structureless statoliths after KMnO<sub>4</sub> fixing doubtless correspond least to the in vivo structure. If one reduces the fixing time from 2 hours [Sievers 1965] to less than 30 minutes (Fig. 7b, 5 min.) then statolith crystallites can also be found after KMnO<sub>4</sub> fixing. The crystallite content thus decreases as fixing time increases. The phenomena described are surprising when one considers the minimal solubility of BaSO<sub>4</sub>.

The following solution tests with synthetic crystallites confirm the fixing results with biogenic crystallites. Figure 9a shows numerous BaSO<sub>4</sub> crystallites in an electron microscope photo. The same section can be seen in Fig. 9b, but after 24 hours of treatment with 2% KMnO<sub>4</sub>. Corresponding to the size of the synthetic crystallites, the exposure time was lengthened in comparison to the fixing time of the rhizoids. The flawed points in individual

ORIGINAL PAGE IS  
OF POOR QUALITY

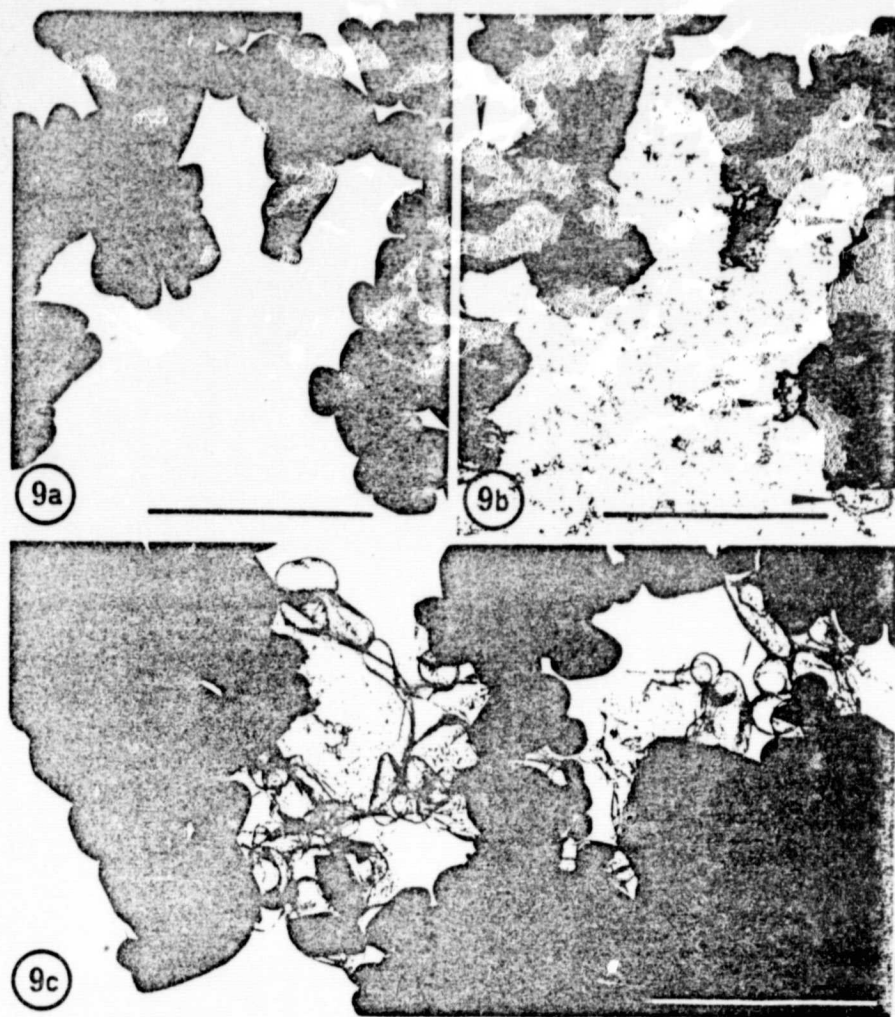


Fig. 9. Solution behavior of synthetic  $\text{BaSO}_4$  crystallites in response to an aqueous solution of 2%  $\text{KMnO}_4$ , 24 hrs. (b) and 2%  $\text{OsO}_4$ , 22 hrs (c). (a) shows the same area as (b), but before treatment with  $\text{KMnO}_4$ . The loss of substance is clear. Only shells are left of some crystallites, resulting from the evaporation of carbon onto them (arrows). In some shells, smaller crystallites are still present (c). Mark =  $1\mu\text{m}$ , 30,000:1.

crystals can be clearly recognized (arrows). Empty shells indicate the original position of the dissolved crystallites. These shells developed during electron irradiation by the evaporation of carbon on the crystallites during the production of control photos. The structures between the crystallites (Fig. 9b) probably involve contaminations by reaction partners coming from the support film. The subsequent Fig. 9c shows synthetic  $\text{BaSO}_4$  crystallites

after 22 hours in 2% OsO<sub>4</sub>. Here too, empty shells bear witness to the partial dissolution of the crystallites. /222

On the other hand, no decrease in the crystallite component can be determined after a 24 hour treatment with glutaraldehyde and acrolein. The composition of this solution corresponds to the fixing solution (cf. Method) used for our studies. /223

Quantitative statements cannot be expected from the solution tests. However, they show clearly that both statolith and BaSO<sub>4</sub> crystallites are attacked by KMnO<sub>4</sub> and OsO<sub>4</sub> solutions, but not by aldehydes. At the same time the differences in the fine structure of the statoliths, as described earlier [Sievers 1967] are explicable.

#### 4. Discussion

The microsound analysis and atomic absorption spectrophotometer, as well as the comparison of the diffraction graphs, show without a doubt that the Chara rhizoid statoliths contain BaSO<sub>4</sub> crystallites. This may be the first confirmation that the element barium plays a functional role in organisms: in the form of barium sulfate it acts as a statolith.

Barium compounds certainly do not belong among the minerals essential for plant nutrition. However, barium has been detected in many lower and higher plants (literature surveys: Bowen and Dymond 1965, Gmelin 1960). While a slight addition of barium salts to the culture medium produces increased growth, Ba<sup>2+</sup> ions in larger concentrations are toxic [Loew 1903; McHargue 1919; Scharrer and Schropp 1937). BaSO<sub>4</sub> crystals with an edge length up to 0.75 μm were discovered in Spirogyra cells [Kreger and Boere, 1969]. The electron microscope pictures of the ethanol-fixed cells permit no recognition of bordering of the crystal space with membranes [loc. cit.]. If the crystals are not placed

in separate compartments the  $Ba^{2+}$  concentration in the entire cytoplasm must be ca. 2 mg/l (ca. 15  $\mu M$ ) corresponding to a saturated barium sulfate solution. Fine structure examinations lead to the hypothesis that the synthesis of biocrystals and biocrystallites generally takes place in special membrane-lined reaction spaces. In addition to the synthesis of barium sulfates in Chara statoliths this also applies to the synthesis of calcium oxalates [Frank and Jensen 1970; Schütz et al. 1970; Horner and Whitmoyer 1972].

The accumulation performance of the statolith compartment is considerable; the  $Ba^{2+}$  concentration of the culture medium (pond water) is under 0.1  $\mu M$ , as our own measurements with the atomic absorption spectrophotometer showed. The barium accumulation mechanism has not yet been examined. The existence of a  $Ba^{2+}$  selective membrane carrier could be postulated. Nothing can be said either about the location or function of such a  $Ba^{2+}$  carrier (selective for a relatively toxic ion!).

As the present results show, in the evaluation of crystal content on the basis of electron microscopy the general solubility of the crystals should be determined; it can also be further increased by an electrolytic effect in the fixing solution [Gmelin 1960]. Among the applied fixatives, aldehydes do not dissociate, in contrast to  $KMnO_4$  and  $OsO_4$ . It could be demonstrated that  $KMnO_4$  and  $OsO_4$  solutions attack the synthetic  $BaSO_4$  crystallites (Fig. 9) while the glutaraldehyde-acrolein solution does not change them. In supplement to earlier studies (Fig. 7a; Sievers 1965) it is also possible to represent statolith crystals after 1224  $KMnO_4$  fixation, but only after significantly shorter fixing times (5 min.; Fig. 7b). We cannot examine in further detail here what role is played by other physico-chemical processes, in addition to electrolyte action, in the preparations for electron microscopy of 7 nm crystallite particles.

This new knowledge demands an examination of earlier inter-



pretations [Sievers 1965, 1967]. The statoliths of older rhizoids, which contain few or no crystallites, must be viewed now as artifacts from fixation. After pure aldehyde fixation the crystallite content of all statoliths in older rhizoids (5 days and more) is about the same. Thus the statoliths are not decomposed, at least so long as the rhizoids are still growing.

The  $\text{BaSO}_4$  crystallites determine the density and thus also the functionality of the "shiny bodies." They are doubtless excellent susceptors for gravitational force. Their density is ca.  $4.5 \text{ g cm}^{-3}$ , compared to  $1.5 \text{ g cm}^{-3}$  for starch. Since  $\text{BaSO}_4$  is chemically almost inert, biochemical interaction with cell compartments, induced by the crystallites, is probably to be ruled out. One can thus assume that the statoliths of Chara rhizoids are active primarily through their mass. Their fibrillary basic substance could possibly serve only as a structural framework for crystallites [Schröter et al., 1973]. No statements can as yet be made about the chemical nature of the substances dissolved in the aqueous phase of the statolith vacuoles. As our experiments showed, they store up neutral red like normal vacuoles.

Under general biological aspects, it is also especially remarkable that the characeids have developed sui generis statolith organelles in the course of their evolution, in contrast to higher plants. Large amyloplasts are present in all cells of the thallus, except the rhizoids, which always contain starch-free and thus unsedimentable plastides.

The authors wish to thank Prof. Dr. H.J. Hühling, Institute for Medical Physics of the University of Münster, for the opportunity to work with the microsound; Dr. P. Nicholson, Münster, for his technical assistance, Prof. Dr. H.R. Oswald and Dr. A. Portmann, Inorganic Chemical Institute of the University of Zurich, for their excellent advice and for producing the diffraction graph of synthetic  $\text{BaSO}_4$ , and Dr. P.D. Peters, Cavendish Laboratory, Cambridge, for discussions on the question of quantitative x-ray microanalysis.

## REFERENCES

- Bowen, H.J.M., Dymond, J.A.: "Strontium and barium in plants and soils," Proc. roy. Soc. B. 144, 355-368 (1955).
- Deloye, F.X., Cador, Ch.: "Méthode simple et pratique pour le dépouillement des microdiffractions." J. Microscopie 15, 99-102 (1972).
- Frank, E., Jensen, W.A.: "On the formation of the pattern of crystal idioblasts in *Canavalia ensiformis* DC. IV. The fine structure of the crystal cells." Planta (Berl.) 95, 202-217 (1970).
- Gmelin: "Barium." In: Handbuch der anorganischen Chemie [Handbook of Inorganic Chemistry] (Ergänzungsband) Weinheim: Chemie 1960.
- Horner, H.T., Jr., Whitmoyer, R.E.: "Raphide crystal cell development in leaves of *Psychotria punctata* (Rubiaceae)" J. Cell Sci. 11, 339-355 (1972).
- Kreger, D.R., Boere, H.: "Some observations on barium sulphate in *Spirogyra*." Acta bot. neerl. 18, 143-151 (1969).
- Lüchli, A.: "Electron probe analysis" In: Microautoradiography and electron probe analysis, p. 191-236, Lüttge, U., ed., Berlin-Heidelberg-New York: Springer 1972.
- Loew, O.: "Einige Bemerkungen zur Giftwirkung der Salze des Magnesiums, Strontiums und Bariums auf Pflanzen," Landwirtschaftl. Jahrb. 32, 509-515 (1903).
- McHargue, J.S.: "Effects of certain compounds of barium and strontium on the growth of plants." J. agric. Res. 16, 183-194 (1919).
- Reimer, L.: Elektronenmikroskopische Untersuchungs- und Präparationsmethoden [Study and Preparation Methods for Electron Microscopy], Berlin-Heidelberg-New York: Springer 1967.
- Scharrer, K., Schropp, W.: "Über die Wirkung von Strontium- und Barium-Ionen auf das Wachstum einiger Pflanzen." Bodenk. u. Pflanzenernähr. 3, 369-385 (1937).
- Schütz, F., Diers, L., Bathelt, H.: "Zur Feinstruktur der Raphidenzellen. I. Die Entwicklung der Vakuolen und der Raphiden." Z. Pflanzenphysiol. 63, 91-113 (1970).
- Schröter, K., Rodriguez-Garcia, M.I., Sievers, A.: "Die Rolle des endoplasmatischen Retikulums bei der Genese der Charastatolithen." Protoplasma (Wien) 76, 435-442 (1973).

- Sievers, A.: "Elektronenmikroskopische Untersuchungen zur geotropischen Reaktion. I. Über Besonderheiten im Feinbau der Rhizoide von Chara foetida." Z. Pflanzenphysiol. 53, 193-213. (1965).
- Sievers, A.: "Elektronenmikroskopische Untersuchungen zur geotropischen Reaktion, II. Die polare Organisation des normal wachsenden Rhizoids von Chara foetida!" Protoplasma (Wien) 64, 225-253 (1967).
- Sievers, A., Schröter, K.: "Versuch einer Kausalanalyse der geotropischen Reaktionskette im Chara-Rhizoid," Planta (Berl.) 96, 339-353 (1971).
- Skaer, R.J., Peters, P.D., Emmines, J.P.: "The localization of calcium and phosphorus in human platelets." J. Cell Sci. 15, 679-692 (1974).
- Zacharias, E.: "Über Entstehung und Wachstum der Zellhaut." Jahrb. wiss. Bot. 20, 107-132 (1889).